International Journal of Applied Earth Observations and Geoinformation 114 (2022) 103065

Contents lists available at ScienceDirect

International Journal of Applied Earth Observations and Geoinformation

journal homepage: www.elsevier.com/locate/jag

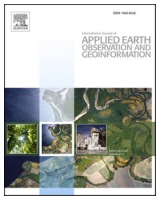

A deep-learning approach for modelling pedestrian movement uncertainty in large- scale indoor areas☆

Wenzhong Shi [a], Yue Yu [a,*], Zhewei Liu [a], Ruizhi Chen [b], Liang Chen [b]

[a] The Department of Land Surveying and Geo-Informatics, The Hong Kong Polytechnic University, 999077, Hong Kong, China
[b] State Key Laboratory of Information Engineering in Surveying, Mapping and Remote Sensing (LIESMARS), Wuhan University, Wuhan 430000, China

ARTICLE INFO

Keywords:
Deep-learning
Pedestrian movement uncertainty
Measurement errors
1D-CNN
LSTM

ABSTRACT

Modelling pedestrian movement uncertainty in complex urban environments is regarded as a meaningful and challenging task regarding the promotion of geospatial data mining and analysis. However, the traditional uncertainty prediction model only takes the movement distance or speed into consideration and is not able to adapt well to time-varying measurement errors. In this paper, a deep-learning framework is proposed for modelling pedestrian movement uncertainty in large-scale indoor areas, in which a hybrid deep-learning model combines a one-dimensional Convolutional Neural Network (1D-CNN) with a long short-term memory (LSTM) network is proposed for enhancing feature extraction performance and reducing time correlation errors. The proposed framework takes human motion related measurement features into consideration, in which the moving step-length and heading information during a time period are also reconstructed and modelled as the input to the deep-learning model. Compared with state-of-art algorithms applied to different real-world trajectory datasets, the proposed deep-learning approach demonstrates much better performance of uncertainty region prediction, including the different indexes (Euclidean error distance, completeness and density) This study has leaded to the provision of an effective and practical framework for modelling trajectory uncertainty of the pedestrian in challenging urban environments, and which is expected to benefit smart city and spatial perception related applications.

1. Introduction

The pedestrian's trajectory data is regarded as the most important feature to better enable the human mobility analysis field, in that it can effectively describe the spatial–temporal movements and social dynamics of an individual or the social activity. With the development of Micro-Electro-Mechanical Systems (MEMS) sensors, various mobile terminals can be applied to provide pedestrian movement information for location based services (LBS), for instance, intelligent transportation systems (Zhu et al. 2019), user habits analyses (Liu et al. 2022), epidemic prevention and control (Shi et al. 2022), and smart healthcare (Pal et al. 2018). Due to the complexity of real-world scenes and the diversity of motion information provided by different mobile equipment, the movement uncertainty of collected pedestrian trajectories has long been considered as an unavoidable problem in the procedure of data acquisition, which can significantly decrease the efficiency and accuracy of knowledge extraction (Shi et al. 2021, Downs et al. 2018). In recent years, how to describe and eliminate the movement uncertainty in large amount of trajectory data in changeable application scenes has increasingly attracted attention, especially regarding the work related to trajectory mining, representation, and spatial query (Chen et al. 2013, Pfoser and Jensen 1999, Yu et al. 2021).

Normally, the collected trajectory in a two-dimensional plane can be described as a finite and time-related dataset of location coordinates $<\mathbf{rt}_1, \mathbf{rt}_2, \ldots, \mathbf{rt}_n>$, provided by various kinds of measurement terminals, where $\mathbf{rt}=\{x, y, t\}$ indicates one of the collected 2D location and corresponding timestamp (Kuijpers et al. 2010). The main factors which cause the uncertainty of the raw trajectory consist of two types: the sampling error and the measurement error. The sampling error represents the discontinuous dataset or a collection of sampling points with

☆ This work was supported by The Hong Kong Polytechnic University (1-ZVN6, 4-BCF7); The State Bureau of Surveying and Mapping, P.R. China (1-ZVE8); and Hong Kong Research Grants Council (T22-505/19-N).

* Corresponding author.
E-mail addresses: Lswzshi@polyu.edu.hk (W. Shi), yue806.yu@connect.polyu.hk (Y. Yu), Jackie.zw.liu@connect.polyu.hk (Z. Liu), ruizhi.chen@whu.edu.cn (R. Chen), l.chen@whu.edu.cn (L. Chen).

https://doi.org/10.1016/j.jag.2022.103065
Received 3 June 2022; Received in revised form 4 October 2022; Accepted 14 October 2022
Available online 20 October 2022

changing sampling rates, in which the motion information between the discontinuous points is unknown (Zheng et al. 2012). The measurement error occurs in the procedure of data collection, related to the positioning approachs applied, the changeable application environments and the deviation of hardware performance (Zheng et al. 2014, Zheng 2015).

The definition of space–time prism (STP) is usually applied in movement uncertainty analysis field to describe the potential path area (PPA) from the collected trajectory database (Miller 1991, Kwan 1998). In previous studies, either the speed or the distance of the moving object is adopted to evaluate the PPA in most scenes, while the performance of uncertainty estimation is limited to the assumption of constant speed, which leads to the overestimated PPA in real-world experiments (Xia et al. 2018, Downs and Horner 2014). To solve this challenge, the researchers explore effective ways to control the influence of speed estimation error added to the PPA prediction, the adaptive speed control criteria is developed to realize a more efficient PPA prediction (Zhou et al. 2018). Apart from the moving speed, the moving distance also proves inevitable effects in the procedure of PPA prediction. Furtado et al. (2018) presented a novel AUB (approximate upper bound) model using the maximum moving distance instead of the adaptive speed to calculate the uncertainty region. In this model, the Manhattan distance is adopted to describe the maximum distance after a comprehensive comparison with the Euclidean distance based method. However, due to the randomness and complexity of pedestrian based movement characteristics and movement routes, the proposed Manhattan distance cannot fully describe the logical relationship between sampling points. In addition, the unstable sampling rate of location information and real-time changing measure error further increase the uncertainty of PPA region prediction.

It can be found from previous works that the existing uncertainty modelling methods mainly focus on the outdoor trajectory uncertainty prediction. Aiming at the pedestrian mobility analysis field, according to the report by the U.S. Environmental Protection Agency, people spend nearly 70 % to 90 % of their time indoors (WEISER 1991), thus the most valuable public trajectories are collected indoors. Compared with the outdoor trajectory, the uncertainty analysis of indoor trajectory has the following challenges and difficulties: 1) The limited reference points: Due to lack of absolute observations such as Global Positioning System (GPS), the collected motion information usually contains limited absolute location reference, which makes it difficult to reconstruct the useful indoor trajectories (Liu et al. 2020); 2) Changing measurement errors of reported indoor locations: Because of complex indoor environments, the real-time collected pedestrian motion information always contains the measurement error that changes with time. The latter should be effectively predicted (Liu et al. 2022); 3) The high complexity of collected pedestrian indoor trajectories: Different from the outdoor network, the pedestrian indoor trajectories are usually disordered because of the randomness of pedestrian indoor movement, this makes it harder to estimate the uncertainty of trajectory (Li et al. 2021).

In this current work, to solve the challenges of uncertainty modelling of indoor trajectories, and focus on developing a unified and continuous model to describe the uncertainty of both sampling error and measurement error by the means of a state-of-art deep-learning approach. Different from establishing the uncertainty region by considering only two adjacent measurement points, this work regards the pedestrian's previous movement period, which contains a series of location points, as a sequence of context. The constructed sequence is further applied as the input vector of a training model to get the current uncertainty prediction result. In addition, the Euclidean distance is adopted as the output value of the training model, and the Euclidean distance coefficient is adaptively selected according to the expected results of the training phase. To establish an effective and compact uncertainty region, this work extracts the various features from the pedestrian's movement information to describe the changeable measurement error and sampling error, the predicted Euclidean distance is finally applied to construct the uncertainty region according to the spatial–temporal comparison results. The comprehensive experiments using generated real-world trajectories datasets prove the effectiveness of the proposed deep-learning based approach, and the comparison results. Further the developed state-of-art algorithms demonstrate the robustness and precision of the proposed approach in the field of modelling movement uncertainty in pedestrian trajectory datasets.

The contributions of this study can be summarized as follows:

(1) Instead of using only reference points for uncertainty analysis, a continuous indoor pedestrian trajectory reconstruction model, which can be applied in the case of large-scaled indoor areas and limited reference points is proposed. The reconstructed trajectory can effectively improve the performance of the raw trajectory and continuity of sparse reference location points.
(2) The study presented in this paper proposes a novel deep-learning model for uncertainty prediction using the combination of 1D-CNN and LSTM networks. Different from the traditional model, a series of location points, during a short time period, are regarded as the influencing factors to precisely describe the time–space relationship of the uncertainty of the pedestrian's trajectory.
(3) The enhanced training dataset generated in a large-scale indoor scene, by adding more complex indoor routes to improve the comprehensiveness of the training dataset, is presented. The enhanced training dataset contains not only the measurement error, but also the sampling error, thus enabling more pedestrian motion information to be collected, hence benefitting the performance of the final uncertainty prediction.
(4) This paper adopts the Euclidean distance to describe the measurement error of each collected trajectory point, the Euclidean coefficient being adaptively selected according to the training result. The final uncertainty region is established by taking both the sampling and measurement errors into consideration, under complex pedestrian motion modes.

The structure of the paper is organized as follows: Section 2 describes the problem definition, dataset preparation, and proposed methodology of this study. Section 3 gives the experiment results, to verify the effectiveness and robustness of the involved chosen method. Section 4 presents the novelties and limitations of our work. Section 5 the conclusions of the study together with the potential applications of our method.

2. Problem statement, Dataset, and methodology

In this section, the main challenges and difficulties of movement uncertainty prediction of large-scaled pedestrian indoor trajectory are discussed and an enhanced dataset is prepared and described for training purposes. Finally, the deep-learning based methodology is proposed to provide a robust and effective approach aiming at solving the stated problems.

2.1. Problem statement

The purpose of the work described in this paper, is to establish a comprehensive and robust model related to pedestrian movement uncertainty in complex and large-scaled indoor areas. Considered are both the sampling and measurement errors. In addition, an adaptive scheme, the aim of which is to change the measurement errors originating from time-related influence factors and location source-related influence factors, is presented. The key definitions related to our problem are given below:

Definition 1. Spatiotemporal point. A spatiotemporal point STP provided by different positioning approaches is a two-dimensional spatial

point with the timestamp, denoted as $STP_i = (x,y,t)$, where (x,y) and t indicate the spatial location point and corresponding timestamp of STP_i.

Definition 2. Ground-truth Trajectory. A ground-truth trajectory $GT = \{GT.STP_1, GT.STP_2, ..., GT.STP_n\}$ is an indexed STP collection representing an individual's actual trajectory. The ground-truth trajectory is usually provided by the high accuracy measurement approaches such as total station or Lidar positioning system.

Definition 3. Reconstructed Trajectory in Large-scaled Indoor Area. A reconstructed trajectory RT is an indexed STP collection representing a trajectory reconstructed from algorithms to approximate an individual's ground-truth trajectory $RT = \{RT.STP_1, RT.STP_2, ..., RT.STP_n\}$, where $RT.STP_n$ is the reconstructed trajectory point corresponds to$GT.STP_n$.

Thus the research problem viz modelling the movement uncertainty of large-scaled indoor trajectories is presented as:

Problems of indoor movement uncertainty:

(1) Unlike outdoor trajectories with continuous GPS-reported location points, the first challenge regarding the indoor trajectory is that the limited reference points are contained within indoor environments, thus a continuous indoor trajectory needs to be reconstructed based on limited reference points.
(2) In addition, based on the ground-truth trajectory GT and reconstructed trajectory RT, the aim is to find the mapping relationship M between GT and RT to Dis($GT.STP_i$, $RT.STP_i$):$M : RT \rightarrow Dis(GT.STP_i, RT.STP_i)$, in which the Dis($GT.STP_i$, $GT.STP_i$) indicates the measured Euclidean distance between $GT.STP_i$ and $RT.STP_i$.
(3) Different from traditional reconstructed GPS trajectories with no timestamp information, indoor reconstructed trajectories RT can obtain a reconstructed point corresponding to every point of the ground-truth trajectory (eg, $RT.STP_i$, $t = GT.STP_i.t$), hence enabling the calculation of the pointwise deviations between $RT.STP_i$ and $GT.STP_i$, also contains the time-related sampling error and measurement error.

2.2. Training dataset generation

Different from the outdoor trajectories provided by the GPS-reported continuous location points with roughly the similar sampling and measurement errors, the collected indoor trajectory always has a changeable sampling error and measurement error. In addition, the raw collected indoor trajectory usually contains limited reference points, which need to be reconstructed to better combine with the human motion information to enable the provision of continuous indoor location points.

The pedestrian indoor trajectory is presented as a graph containing the reference points and motion information, and is shown in Fig. 1:

Shown in Fig. 1 is the procedure of the indoor trajectory reconstruction, in which the pedestrian motion information contains both calculated step-length and heading values between two different spatiotemporal points. The location of the reference points is provided by the absolute location sources such as Wi-Fi stations, BLE nodes, and QR codes.

By using the motion information collected during the trajectory period, the total indoor trajectory can be reconstructed as:

$$STP_i(\mathrm{L_i}, \theta_i) = \mathbf{R}_{01} + \sum_{i=1}^{n} \begin{bmatrix} \mathrm{L_i}\cos(\theta_i) \\ \mathrm{L_i}\sin(\theta_i) \end{bmatrix} \quad (1)$$

In which $\boldsymbol{R}_{01}$ indicates the first reference point in the selected trajectory. L_i and θ_i represent the collected step-length and heading information between two adjacent spatiotemporal points. The latter can be estimated by Yu et al. (2020).

In this aspect of the study, to further improve the performance of indoor trajectory reconstruction, the equation (1) is regarded as the optimization problem:

$$\xi(L_i, \theta_i) = (z - STP_i(\mathrm{L_i}, \theta_i))^{\mathrm{T}} \boldsymbol{\rho}^{-1} (\mathbf{z} - \mathrm{STP_i}(\mathrm{L_i}, \theta_i)) \quad (2)$$

where $\boldsymbol{\rho}$ indicates the covariance matrix of the measured value.

Hence, the aim of the graph-based trajectory optimization is to find the minimum state vector of the above function:

$$(L_i, \theta_i)^* = \underset{L_i, \theta_i}{\operatorname{argmin}} \xi(L_i, \theta_i) \quad (3)$$

where (L_i, θ_i) is a vector of collected step-length and heading, which reaches the optimal value when the optimal function $\xi(L_i, \theta_i)$ is acquired using the Gradient Descent (GD) method proposed by Yu et al. (2022).

After obtaining the optimized reconstructed indoor trajectory, the ground-truth trajectory is then required. In this work, the raw sensors data is provided by the IPIN-2018 track 3 competition dataset (Renaudin et al. 2019), and the reference points are provided by the total station, with centimeter-level accuracy, and with each ground-truth trajectory being constructed using a number of 5 ~ 8 reference points. According to previous work it has been found that an overall accuracy of 0.1 ~ 0.3 m is able to be acquired (Liu et al. 2022). In the enhanced dataset, more trajectories were collected from large-scaled indoor scenes and with more complex walking routes. On average, each data vector in the constructed dataset contains the following values:

$$Vector_{train} = \{x_{G/O}, y_{G/O}, L, \theta, x_r, y_r\} \quad (4)$$

where $x_{G/O}$ and $y_{G/O}$ indicate the ground-truth coordinate or the reconstructed coordinate, L and θ represent the step-length and heading information, x_r and y_r are the raw coordinates of the trajectory.

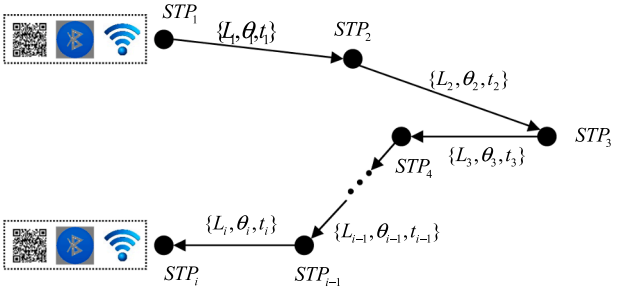

Fig. 1. Description of Indoor Trajectory reconstruction.

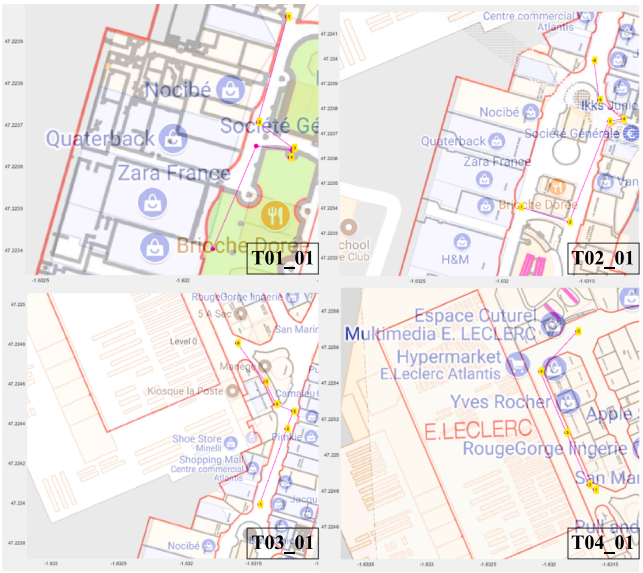

Fig. 2. Walking Routes of the Collected Dataset.

Parts of the walking routes in the generated dataset are shown in Fig. 2, and the reference walking routes and corresponding control points are described in the indoor map using pink and yellow markers:

2.3. Movement uncertainty features extraction

In order to comprehensively describe the relationship between the movement uncertainty index and the reconstructed trajectory, the following features were extracted from the latter to identify the mapping relationship between the reconstructed trajectory and uncertainty index of each spatiotemporal point:

(1) Estimated step-length value L_i between two adjacent spatiotemporal points.
(2) Estimated heading value θ_i between two adjacent spatiotemporal points.
(3) Estimated coordinate update interval $\Delta\kappa_i$ between two adjacent spatiotemporal points.
(4) Estimated step number $step(i)$ at current timestamp.
(5) Estimated walking speed v_i between two adjacent spatiotemporal points:

$$v_i = \frac{L_i}{\Delta\kappa_i} \tag{5}$$

(6) Current recorded distance:

$$Dis_{cum}(i) = \sum_{i=1}^{k} L_i \tag{6}$$

(7) Progress indicator of current distance and overall distance:

$$PI_d(i) = \frac{\sum_{i=1}^{k} L_i}{\sum_{i=1}^{n} L_i} \tag{7}$$

where n represents the overall number of steps during in selected trajectory, k represents the current steps happened.

(8) Progress indicator of current used time and overall time period:

$$PI_t(i) = T(i)/T_{total} \tag{8}$$

where T_{total} represents the recorded time period of selected trajectory,$T(i)$ represents the used time period at the current moment.

(9) Progress indicator of current steps quantity and the overall step quantity:

$$PI_s(i) = step(i)/step_{total} \tag{9}$$

where $step_{total}$ represents the overall step quantity of the estimated trajectory,$step(i)$ indicates the current counted step quantity.

(10) Estimated heading variation $\Delta\theta_i$ between two adjacent spatiotemporal points:

$$\Delta\theta_i = \theta_i - \theta_{i-1} \tag{10}$$

(11) Cumulative heading changes compared with the first timestamp:

$$\Delta\theta_i = \sum_{i=1}^{k} (\theta_i - \theta_1) \tag{11}$$

The above features can effectively describe the performance of the selected indoor trajectory and the corresponding uncertainty index. The extracted features are further modelled as the input vector of the deep-learning based uncertainty prediction framework.

In addition, the proposed deep-learning based uncertainty prediction model fully consider the sampling error and measurement error, in which the estimated coordinate update interval $\Delta\kappa_i$ between two adjacent spatiotemporal points and the continuous time period related input vector are applied to solve the problem of the sampling error, and the other extracted features extracted from the trajectory are applied to solve the problem of the measurement error.

2.4. Proposed deep-learning based uncertainty prediction

In this section, a hybrid deep-learning structure combining the 1D-CNN and LSTM models is applied for uncertainty analysis, which comprehensively considers both the time and feature correlations of the large-scaled indoor trajectory. To solve the problem of the time correlation of the indoor trajectory, the LSTM network is effective as regards the consideration of the before-and-after correlation of the trajectory data, usually applied in such as the fields of text generation, machine translation, speech recognition, generating image descriptions and video tagging (Shu et al. 2020). In the study presented in this Paper, rather than simply considering the mapping relationship of adjacent coordinates, the trajectory data, over a period of time, will be seen as a complete unit to present the prediction of uncertainty during a current moment.

In the previous work proposed by Liu et al. (2022), a typical LSTM network is applied for uncertainty modeling of indoor trajectories, and five different features extracted from the trajectories are modeled as the input feature of LSTM. The problems are that the indoor trajectories are usually complex, and more features are required in order to comprehensively describe the performance of the overall trajectory, the single LSTM network cannot realize good feature extraction of indoor trajectories. Thus, in this work, the 1D-CNN model is connected before LSTM network to provide more robust features extraction ability. In addition, to realize the better performance of uncertainty analysis in large-scale indoor areas, an enhanced dataset contains indoor trajectories that cover more complex walking routes are required for training purposes to improve the universality of final uncertainty prediction model.

Additional features are required to enable the presentation of a description of the selected trajectory. In section C, the number of 11 features are extracted and used to solve the feature correlation problem of uncertainty regarding indoor trajectory predictions. In order to better learn and extract the feature vector used to describe the trajectory, the 1D-CNN model is applied before the LSTM network for feature learning and extraction. The 1D-CNN model can be well applied to the time series analysis of one-dimensional data; to analyze signal data with a fixed length period and also, to natural language processing tasks (Yu et al., 2022).

To combine the advantages of both 1D-CNN and LSTM models and also to consider the time correlation and feature correlation of the large-scaled indoor trajectory, a hybrid deep-learning structure is proposed in this study, using the combination of 1D-CNN and LSTM networks, described in Fig. 3:

In the convolution layer, the relationship between input value and output value is described as:

$$y_j = \zeta\left(\sum_{i=1}^{M} x_i * k_{ij} + b_j\right) \tag{12}$$

where x_i indicates the input vector, k_{ij} indicates the kernel weights, b_j indicates the biases, $\zeta(\cdot)$ represents the activation function, y_j is the output vector of the convolution layer.

In the LSTM layer, the update model of LSTM parameters is described as:

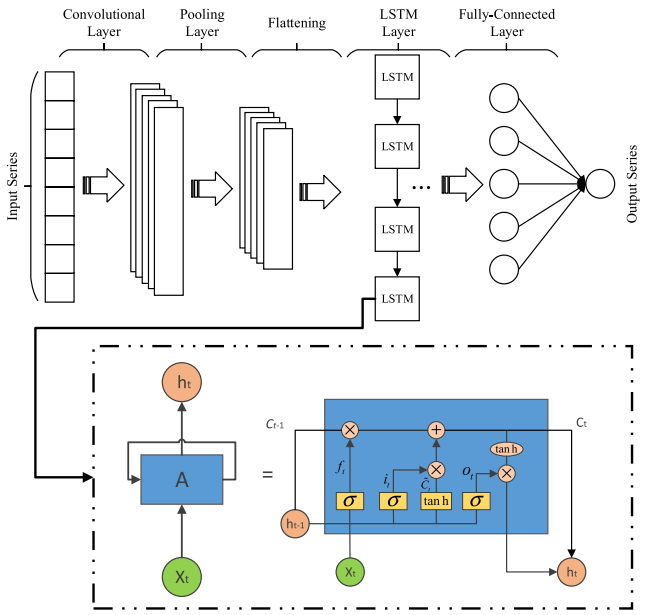

Fig. 3. Deep-learning Structure of 1D-CNN and LSTM.

$$\begin{cases} f_t = \sigma\cdot(W_f\cdot[h_{t-1}, X_t] + b_f) \\ i_t = \sigma\cdot(W_i\cdot[h_{t-1}, X_t] + b_i) \\ \widetilde{C}_t = \tanh\cdot(W_C\cdot[h_{t-1}, X_t] + b_C) \\ o_t = \sigma\cdot(W_o\cdot[h_{t-1}, X_t] + b_o) \\ h_t = o_t\cdot\tanh(C_t) \end{cases} \tag{13}$$

where i_t,f_t,o_t represent the input, forget and output units,X_t indicates the input vector of LSTM model at the timestamp t, and the h_t represents the hidden state vector, regarded as the output of the LSTM model at that moment.σ indicates the sigmoid function, and C_t is the candidate vector which is combined with output vector as the memorized state at timestamp t.

Finally, the output layer of LSTM units is modelled as the input vector of a fully-connected network function $MLP(\cdot)$ and the predicted uncertainty error and is presented as:

$$\widehat{E}_i = MLP(y_i) \tag{14}$$

The Euclidean distance is adopted to describe the measurement error of each collected trajectory point and mean squared error as the loss function, in order to evaluate the difference between the predicted uncertainty error $\widehat{E}_i$ and ground-truth error $Dis(GT.P_i, RT.P_i)$.

3. Experimental Results

Given in the following section, is a comprehensive comparison between the proposed deep-learning structure and state-of-art approaches. In addition, an enhanced dataset is developed and presented, for the better performance of the final uncertainty prediction. This dataset contains more comprehensive training trajectories, while different accuracy indexes are applied for evaluating the performance of uncertainty prediction of large-scaled indoor trajectories.

3.1. Dataset preparation and parameter settings

In the headlined work, the raw sensors data and locations of reference points are provided based on the IPIN-2018 training dataset, in which the original data is collected in a multi-floor contained indoor shopping mall in Nantes, France. The ground-truth trajectory is estimated using the optimization results of raw trajectory and high-accuracy control points, which have been described in Section 2. The trajectory comparison and uncertainty error comparison between reconstructed trajectory (RT) and ground-truth trajectory (GT) is shown in Fig. 4:

Details in Fig. 4 indicate that the reconstructed trajectory has a significant difference from the ground-truth trajectory. In the previous dataset proposed by Liu et al. (2022), 18 indoor trajectories, containing ground-truth references and reconstructed references have been provided, regarding the enhanced dataset in this work, the additional 12 indoor trajectories which cover more comprehensive and complex indoor walking routes to acquire a better performance of the uncertainty prediction of large-scaled indoor trajectories.

The overall parameters of the enhanced training dataset are summarized in Table 1:

It is seen in Table 1 that the enhanced dataset prepared for this work contains over 30 trajectories and 6526 spatiotemporal points. The average length of trajectory reaches 121.3 m, with 123.8 s average time period. In addition, the collected trajectories have different sampling intervals due to the changeable step period.

In the proposed deep-learning framework, the 1D-CNN, LSTM, and fully-connected network are combined to integrate the advantages of each. For the presented model setting, the Adam, because of its efficiency regarding a large amount of training dataset, is applied as the optimizer. The dimension of the input vector of the deep-learning structure is set as 11, and the dimension of the output hidden state from the last unit is set as 30. Sensitivity analysis indicates that the above settings can, in general, effectively reflect the model's average performance when using different settings.

To realize the training purposes of the proposed deep-learning framework, we randomly selected 70 % of 6526 spatiotemporal points collected from 30 trajectories as the training dataset and remained 30 % as the test dataset. After the training phase, the trained uncertain prediction model will be applied for the evaluation of the test dataset and statistics the final uncertainty prediction accuracy.

3.2. Accuracy comparison with LSTM model

In previous work proposed by Liu et al. (2022), a novel LSTM network has been proposed for uncertainty analysis of indoor trajectory. The limitations of a single LSTM model are that the LSTM model just considers the time correlation, to improve the performance of feature correlation of the proposed model, hence the 1D-CNN has been applied to enhance the ability of feature learning. ‘

The main objective of the following section is section to compare the uncertainty prediction accuracy between the single LSTM model in the previous work of the authors and the hybrid deep-learning (HDL) model in the current work. During the comparison procedure related to different uncertainty prediction models, the previous dataset (PD) and enhanced dataset (ED) are compared. To do so, the uncertainty estimation error of each trajectory is statistically analyzed as one complete identity, while the **Euclidean error distance** index calculated between positioning error originated from the optimized trajectory and positioning error provided by HDL model is applied as the reference standard for the uncertainty prediction, the predicted results using different models and datasets are compared in Table 2 and Fig. 5:

It can be seen from Table 2 and Fig. 5 that the enhanced dataset provides a better performance regarding indoor trajectory uncertainty prediction when using the same trained model. In addition, the proposed HDL structure further improves the performance of the uncertainty prediction of the indoor trajectory when compared with the performance of the single LSTM model, by using the combination of 1D-CNN and LSTM network, and uses more features extracted from indoor trajectories for realizing more accurate uncertainty prediction results. For the PD, the proposed HDL model realizes the error prediction accuracy ranged from 0.67 m to 0.88 m, compared with the LSTM model ranged from 1.26 m to 1.45 m. For the ED, the proposed HDL model realizes the error prediction accuracy ranged from 0.46 m to 0.68 m, compared with the LSTM model ranged from 0.94 m to 1.25 m. In addition, the

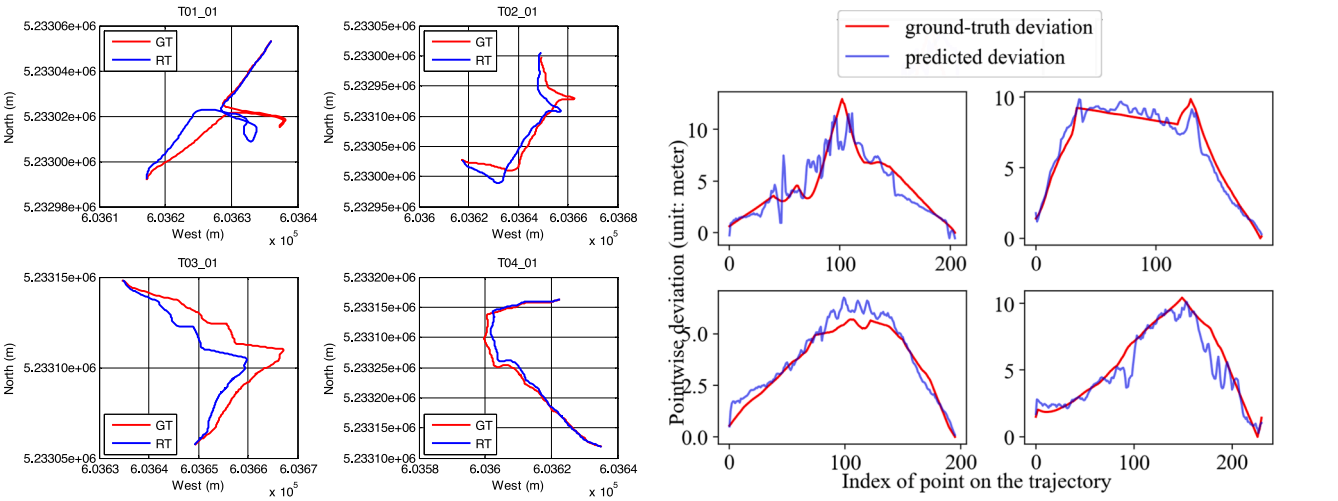

Fig. 4. (a) Comparison Between RT and GT. (b) Deviation Error Between RT and GT.

Table 1
Parameters of Enhanced Dataset.

Number of Trajectories	Number of Location Points	Average Trajectory Length	Average Time Period	Largest Walking Speed	Average Sampling Interval
30	6526	121.3 m	123.8 s	4.94 m/s	0.57 s

Table 2
Accuracy Comparison Between Different Models and Datasets.

Traj No.	LSTM (PD)	LSTM (ED)	HDL (PD)	HDL (ED)
T01_01	1.38 m	1.04 m	0.72 m	0.61 m
T01_02	1.33 m	1.07 m	0.82 m	0.58 m
T01_03	1.31 m	0.99 m	0.67 m	0.67 m
T02_01	1.36 m	1.04 m	0.69 m	0.54 m
T02_02	1.33 m	1.18 m	0.88 m	0.55 m
T02_03	1.43 m	1.09 m	0.75 m	0.59 m
T03_01	1.29 m	1.11 m	0.77 m	0.62 m
T03_02	1.26 m	1.24 m	0.85 m	0.57 m
T03_03	1.34 m	1.15 m	0.75 m	0.54 m
T04_01	1.45 m	1.15 m	0.77 m	0.62 m
T04_02	1.28 m	1.23 m	0.69 m	0.57 m
T04_03	1.31 m	1.13 m	0.86 m	0.59 m
T05_01	1.44 m	1.25 m	0.83 m	0.65 m
T05_02	1.39 m	0.94 m	0.67 m	0.62 m
T05_03	1.28 m	1.12 m	0.86 m	0.57 m
T06_01	1.41 m	1.16 m	0.73 m	0.53 m
T06_02	1.31 m	1.02 m	0.74 m	0.61 m
T06_03	1.29 m	1.09 m	0.83 m	0.66 m
T07_01	–	1.14 m	–	0.58 m
T07_02	–	1.05 m	–	0.54 m
T07_03	–	1.04 m	–	0.68 m
T08_01	–	1.23 m	–	0.51 m
T08_02	–	1.05 m	–	0.46 m
T08_03	–	1.14 m	–	0.63 m
T09_01	–	1.04 m	–	0.49 m
T09_02	–	1.11 m	–	0.55 m
T09_03	–	0.99 m	–	0.66 m
T10_01	–	1.25 m	–	0.59 m
T10_02	–	1.01 m	–	0.53 m
T10_03	–	1.17 m	–	0.61 m
Average	1.34 m	1.11 m	0.77 m	0.58 m

proposed HDL model significantly improves the performance of error prediction under each evaluated trajectory compared with LSTM model, and the increment rate of each track is also different mainly due to the different pedestrian movement patterns and the complexity of the movement route and distance under each trajectory. Notably, the

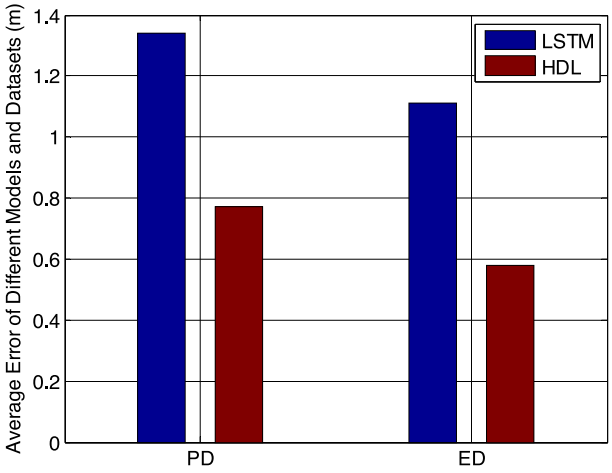

Fig. 5. Average Errors of Different Models.

average prediction error was enabled to decrease from 1.11 m to 0.58 m.

3.3. Indexes comparison of completeness and density

In this section, three state-of-the-art uncertainty prediction models are compared with those which have been proposed. In these models, **completeness** and **density** indexes are adopted as the reference standards for the uncertainty prediction of each trajectory under the same dataset for comprehensive evaluation of different models. The **completeness** index is proposed to describe the overall coverage of ground-truth trajectory using generated uncertainty region, which is effective for evaluating the degree of general completion of proposed uncertainty prediction framework. The **density** index is proposed to further calculate the ratio between the total area of the generated uncertainty region and the covered spatiotemporal points from the ground-truth trajectory, which is more fine-grained than the **completeness** index. Thus, two indexes are combined for comprehensively evaluating the performance of our proposed deep-learning based uncertainty prediction algorithm.

Together with the LSTM model using data-driven approach, proposed by Liu et al. (2022), a further three traditional uncertainty prediction models are also compared:

(1) A traditional upper bound (UB) model, the purpose of which is to generate the region of uncertainty by considering the starting/

ending points of the selected trajectory and further, define an error ellipse by using both the period and maximum speed as the effect factors (Lu et al. 2016, Li et al. 2018).

(2) An approximate upper bound (AUB) model, the purpose of which is to generate the uncertainty region by using the constrained error ellipse with the application of "Approximate Upper Bound Distance" (Furtado et al. 2018).

(3) A broad adaptive error ellipse (BAEE) model, which extends the AUB model, by introducing the Minkowski distance metric for model enhancement. The maximum speed for UB is set as 4.94 m/s, (refer to Table 1), and the Minkowski coefficient p-value for error ellipse generation in the BAEE model is set as 1.5. The above methods are used to enable comparisons, given that all three algorithms are applied for uncertainty analysis and uncertainty region generation by Shi et al. (2021).

To comprehensively evaluate the performance of each approach, the uncertainty area, generated by the UB model, is applied as the reference baseline, and the proportional coverage of the ground-truth trajectory points aligned to the constructed uncertainty region. At the beginning and ending points of each optimized trajectory, the measurement error is smaller than other location points because of the high-accurate reference points, thus the uncertainty error of beginning and ending points is set as the accuracy of reference points 0.3 m. The latter provides the **completeness** index of the proposed uncertainty prediction model. In addition, the **density** of covered ground-truth trajectories is an important index, which also presents the precision of the generated uncertainty region.

By taking the consideration of both the **completeness** and **the density** indexes, five different uncertainty prediction models are compared. For the HDL method proposed in this paper, the final uncertainty region is generated based on the combination of a single uncertainty region generated at each coordinate point. The HDL model provides a robust uncertainty prediction result at the location of each spatiotemporal point using the extracted features from a period of pedestrian motion data, in which each spatiotemporal point contains a standard circular uncertainty region and the final generated uncertainty region of the whole trajectory is the union of all the spatiotemporal points from the trajectory. Because our proposed HDL model uses a period of trajectory data to predict the uncertainty value at the current moment, thus, the uncertainty value is set as a higher accuracy at the beginning of the trajectory, the same as the location error of the deployed control point. The typical generated uncertainty region using our proposed HDL algorithm is described in Fig. 6:

It is seen in Fig. 6 that, in general, the proposed HDL algorithm can comprehensively predict the uncertainty region of the large-scaled indoor trajectories, which comprehensively considers both completeness and density indexes and achieve balanced performance.

For the comparison of ellipse models proposed by the UB, AUB, and BAEE models, the same method applied in previous studies are seen to have been used (Liu et al. 2022). The generated uncertainty region of the traditional UB model is much larger than that of other approaches, which are further applied as the reference baseline of other models. The uncertainty region comparison using UB, AUB, BAEE, and proposed HDL is shown in Fig. 7:

It is seen in Fig. 7 that the proposed HDL realizes a higher **completeness** index of uncertainty region prediction of selected trajectories (93 %), compared with the UB (100 %), AUB (69 %), and BAEE (86 %). Regarding the **density** index, the results show that using downsampled trajectory points, the realized density index of HDL is 0.15/m^2, compared with BAEE (0.11/m^2), AUB (0.14/m^2), and UB (0.02/m^2), and acquire comprehensively better uncertainty region prediction performance by considering both **completeness** and **density** indexes.

In addition, a comprehensive comparison between the proposed HDL structure and state-of-art four approaches: UB, AUB, BAEE, and LSTM, using the enhanced dataset (ED) with 30 whole indoor trajectories, is

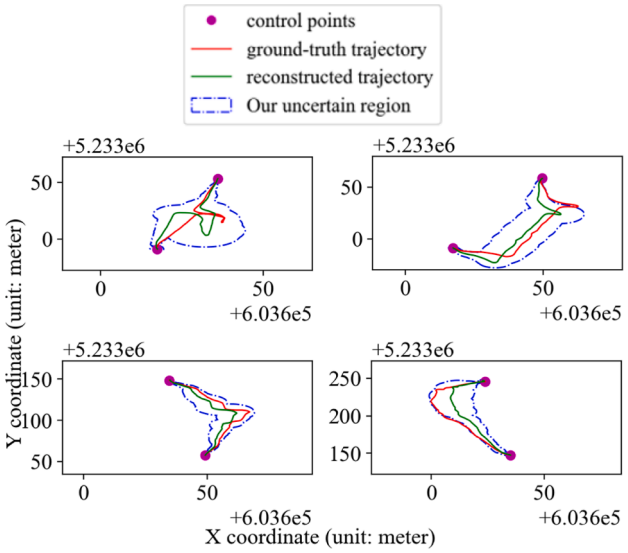

Fig. 6. Generated Uncertainty Region of HDL.

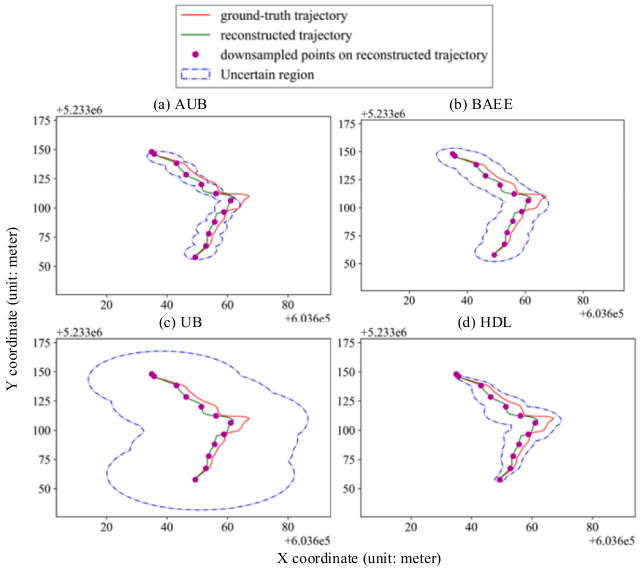

Fig. 7. Comparison of Generated Uncertainty Regions.

made. The uncertainty prediction approaches are divided into classical algorithms (UB, AUB, BAEE) and deep-learning algorithms (LSTM, HDL). The comparison results are described in Table 3:

It is seen in Table 3 that the LSTM based uncertainty prediction provide higher precision compared with that of UB, AUB, BAEE, by using the enhanced dataset. Particularly, the results marked in bold present several trajectories with the most obvious improvement using proposed HDL model, compared with the LSTM model, which are presented in Fig. 8. In general, the proposed HDL approach further improves the performance of overall uncertainty prediction, and the average **completeness** and **density** indexes comparison of five different algorithms is described in Table 4:

Table 4 gives a comprehensive comparison of the average **completeness** and **density** indexes of four existing algorithms and our proposed HDL framework. It can be found that deep-learning algorithms (LSTM, DHL) provide higher accuracy and adaptability compared with the more classical algorithms (UB, AUB, BAEE) regarding both **completeness** and **density** indexes using enhanced dataset (ED), while the HDL algorithm further increases the performance of the uncertainty

Table 3
Performance Comparison of completeness and density indexes.

Traj	UB (ED)		AUB (ED)		BAEE (ED)		LSTM (ED)		HDL (ED)	
No.	Complete-ness (%)	Density (/m^2)	Complete-ness (%)	Density (/m^2)	Complete-ness (%)	Density (/m^2)	Complete-ness (%)	Density (/m^2)	Complete-ness (%)	Density (/m^2)
T01_01	100	0.008	74.5	0.158	100	0.131	100	0.251	96.8	0.288
T01_02	100	0.015	68.3	0.192	100	0.153	99.5	0.222	99.5	0.199
T01_03	100	0.028	71.2	0.140	100	0.122	99.5	0.163	100	0.147
T02_01	100	0.028	82.9	0.148	93.8	0.101	92.2	0.106	97.9	0.107
T02_02	100	0.027	82.5	0.158	92.1	0.107	86.2	0.106	98.4	0.127
T02_03	100	0.024	84.5	0.158	92.3	0.105	98.3	0.139	97.8	0.139
T03_01	100	0.031	42.0	0.135	79.7	0.125	89.2	0.182	95.2	0.206
T03_02	100	0.027	81.6	0.189	100	0.119	100	0.231	99.5	0.256
T03_03	100	0.032	51.0	0.148	88.0	0.116	92.3	0.201	85.1	0.197
T04_01	100	0.034	94.8	0.217	100	0.124	94.8	0.248	99.6	0.279
T04_02	100	0.031	51.1	0.126	67.5	0.089	99.1	0.165	85.3	0.160
T04_03	100	0.031	92.7	0.199	100	0.120	99.1	0.261	100	0.349
T05_01	100	0.029	43.0	0.086	56.6	0.067	89.5	0.108	98.2	0.123
T05_02	100	0.031	44.5	0.091	66.4	0.080	99.2	0.130	97.1	0.126
T05_03	100	0.026	41.9	0.086	57.7	0.069	99.6	0.123	99.1	0.124
T06_01	100	0.011	84.9	0.170	94.4	0.118	93.7	0.177	98.0	0.262
T06_02	100	0.038	100	0.191	100	0.121	89.9	0.200	93.9	0.383
T06_03	100	0.006	59.6	0.144	73.8	0.099	96.3	0.114	96.6	0.117
T07_01	100	0.016	41.0	0.136	88.5	0.163	92.3	0.137	98.1	0.155
T07_02	100	0.012	59.3	0.184	85.6	0.141	72.5	0.121	95.8	0.135
T07_03	100	0.026	64.4	0.140	96.8	0.116	60.7	0.185	88.7	0.248
T08_01	100	0.030	90.6	0.200	100	0.120	90.6	0.255	93.7	0.278
T08_02	100	0.024	70.4	0.119	100	0.108	70.4	0.216	94.2	0.303
T08_03	100	0.021	99.2	0.142	100	0.089	100	0.390	100	0.431
T09_01	100	0.023	100	0.173	100	0.104	99.3	0.249	100	0.256
T09_02	100	0.028	100	0.151	100	0.100	100	0.354	95.2	0.446
T09_03	100	0.025	100	0.165	100	0.101	100	0.373	88.1	0.626
T10_01	100	0.028	50.5	0.097	70.0	0.080	95.2	0.104	93.8	0.109
T10_02	100	0.025	40.2	0.063	62.2	0.062	96.7	0.066	90.5	0.062
T10_03	100	0.021	71.5	0.189	96.3	0.175	95.9	0.264	98.4	0.309

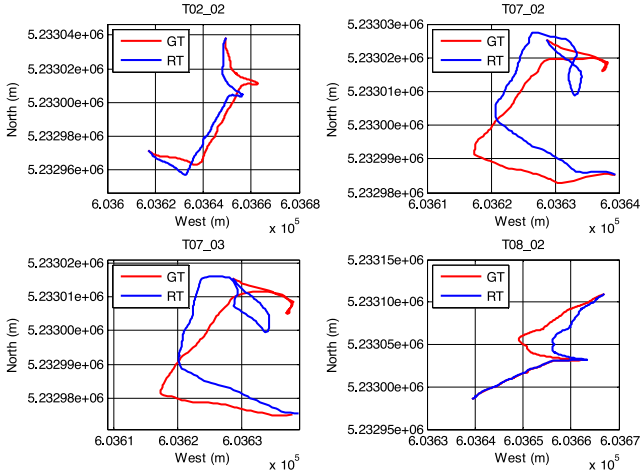

Fig. 8. Four Most Visibly Improved Trajectories.

Table 4
Comparison of Average Completeness and Density Indexes.

Indexes	UB	AUB	BAEE	LSTM	HDL
Completeness (ED)	100	70	87.7	92.6	95.6
Completeness (ND)	100	68.6	86.2	91.5	94.9
Density (ED)	0.021	0.147	0.107	0.159	0.174
Density (ND)	0.019	0.142	0.105	0.154	0.171

prediction of LSTM model, with improvement ratio of **completeness** and **density** indexes of 3.2 % and 9.4 %, respectively.

Finally, we evaluate the dependency of our proposed HDL framework under a new generated test dataset (ND), in which the ground-truth trajectories are provided by the centimeter-level Lidar backpack indoor mapping system (Bao et al. 2022), and a number of 20 test trajectories with an average time period of 2 min are collected under a large-scale office building. Also we compared the average **completeness** and **density** indexes using five different uncertainty prediction models, the comparison results are described in Table 4 and Fig. 9:

It can be found from Fig. 8 that the proposed HDL model maintains the robustness and accuracy of uncertainty prediction, the final evaluated **completeness** and **density** indexes prove highest performance compared with the other four algorithms, including UB, AUB, BAEE, and LSTM. As for the **completeness** index, the proposed HDL realizes an average accuracy of 94.9 %, compared with the other four algorithms with precisions of 100 %, 68.6 %, 86.2 %, and 91.5 %, respectively. As for the **density** index, the proposed HDL realizes an average accuracy of 0.171/m^2, compared with the other four algorithms with precisions of 0.019/m^2, 0.142/m^2, 0.105/m^2, and 0.154/m^2, respectively. In conclusion, the proposed deep-learning based uncertainty prediction model proves stable and accuracy uncertainty prediction performance, which also does not depend on the characteristics of the specific datasets and test environments.

4. Discussion on Contributions and Limitations of Proposed Deep-learning Structure

In this section, the contributions and limitations of our proposed uncertainty prediction framework is presents, and we also point out the future work.

4.1. Contributions of proposed structure

This work presented in this Paper, proposes a novel deep-learning based framework for indoor pedestrian movement trajectory modelling and uncertainty region prediction. The latter is aimed at contributing to the enablement of significant contributions in various

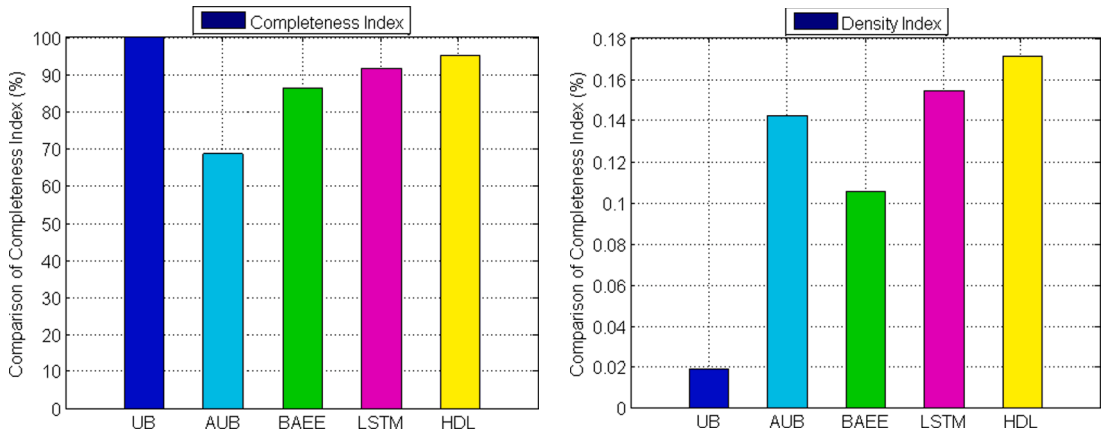

Fig. 9. (a) Comparison of Completeness Index. (b) Comparison of Density Index.

application fields:

Firstly, this paper presents the development of an accurate and effective way for indoor trajectory modelling using daily-life mobile sensing data provided by the public, and presents high granularity based uncertainty prediction results during each step period, with the latter making a significant contributions to mobile applications, such as indoor network reconstruction (Zhou et al. 2021), autonomous indoor navigation database generation (Yu et al. 2021), and public motion data mining (Hwang and Jang 2017). The uncertainty of such public trajectories is essential for the realization of final indoor location based services.

Secondly, the proposed HDL model comprehensively takes the pedestrian's motion features and time-related features into consideration, using a period of mobile sensing data rather than the data acquired from only two adjacent time periods, which realizes much higher uncertainty prediction accuracy compared with traditional models and has a much better error evaluation performance compared with previous work.

Thirdly, from the theoretical level, this newly presented work is regarded as an advanced attempt at modelling the indoor trajectories' potential path area (PPA), by taking both changeable sampling error and measurement error into consideration. It is of note that the traditional approaches only consider the constant sampling error or the measurement error. Much better **completeness** and **density** indexes are achieved compared with the four traditional algorithms which use a real-world dataset, hence benefitting various indoor location based applications such as indoor pedestrian behavior analysis (Ridel et al. 2018), indoor contact tracking of COVID-19 (Munzert et al. 2021), smart healthcare and elderly care (Gogate and Bakal, 2016).

4.2. Limitations of proposed structure

The proposed HDL-based pedestrian indoor movement uncertainty also has limitations as regards real-world applications in complex urban environments., Contained are the following aspects:

Firstly, the pedestrians' daily-life trajectories usually involve both indoors and outdoors. In outdoor areas, Global Navigation Satellite System (GNSS) can also provide continuous location information. Thus, except for considering the indoor motion features of pedestrians, the seamless localization trajectory is also an important application direction and a more comprehensive model is required by taking both indoor and outdoor trajectory features into consideration.

Secondly, the performance of final uncertainty prediction is affected by the input features and capacity, and more trajectory-related features are required to enhance the training dataset performance of final uncertainty region prediction. In addition, the labeling accuracy of the training dataset also affects the training performance accuracy because the ground-truth trajectory is usually difficult to acquire in indoor areas due to the missing of accurate GNSS signal Thus, in such cases, unsupervised learning is a training method that can be explored to autonomously, better enable learning of the uncertainty-related trajectory features and the acquisition of the optimal model.

Thirdly, there are many other location sources in the indoor environment, which contain such as rich wireless signals and magnetic field information. These observations can also be served as constraints for indoor trajectory optimization and uncertainty error prediction. Therefore, the following goal of the newly suggested uncertainty prediction framework is to comprehensively integrate the rich features provided by different indoor location sources and thereby, enhance the performance of uncertainty region prediction by providing more observations. In addition, the relationships between features extracted from different location sources also needs to be considered in our further algorithm, which is different from single location sources acquired from this work, and more input features and the corresponding relationships between different extracted features need to be modeled for better prediction of uncertainty region.

5. Conclusion

Human indoor mobility trajectory plays an important role in the fields of smart city and smart travel based application, while the uncertainty of indoor human mobility trajectory has a significant influence among the final analysis results of large-scaled spatiotemporal data regarding an urban city. The traditional uncertainty prediction models normally consider the constant sampling error or the measurement error, neither is always effective in real-world applications.

A novel deep-learning framework is proposed in this paper in order to realize accurate uncertainty region predictions of pedestrian movement trajectories in large-scale indoor areas. In such cases, both sampling error and measurement error are considered, and the multiple features extracted from public daily life trajectories are adopted as the major vector of the proposed HDL framework. In addition, the proposed model has achieved a strong level of adaptability by considering a period of measured values rather than only adjacent data. The enhanced training data set applied during this study, was collected in large-scale real-world indoor areas, while the robust uncertainty prediction accuracy is expressed by the three important indexes: **Euclidean error distance** (<0.58 m), **completeness** (>95.6 %) and **density (**>0.174 / m^2**)**, which can benefit various mobile applications related to the trajectories estimation.

CRediT authorship contribution statement

Wenzhong Shi: Conceptualization, Methodology, Software, Validation, Formal analysis, Writing – original draft, Writing – review &

editing, Supervision, Project administration, Funding acquisition. **Yue Yu:** Conceptualization, Methodology, Software, Validation, Formal analysis, Writing – original draft, Writing – review & editing. **Zhewei Liu:** Conceptualization, Methodology, Validation, Formal analysis. **Ruizhi Chen:** Supervision, Project administration, Methodology, Writing – review & editing. **Liang Chen:** Project administration, Writing – review & editing.

Declaration of Competing Interest

The authors declare that they have no known competing financial interests or personal relationships that could have appeared to influence the work reported in this paper.

Data availability

Data will be made available on request.

References

Bao, S., Shi, W., Chen, P., et al., 2022. A systematic mapping framework for backpack mobile mapping system in common monotonous environments. Measurement 197 (2022), 111243–112156.

Chen, B.Y., et al., 2013. Reliable space–time prisms under travel time uncertainty. Ann. Assoc. Am. Geogr. 103 (6), 1502–1521.

Downs, J.A., Horner, M.W., 2014. Adaptive-velocity time-geographic density estimation for mapping the potential and probable locations of mobile objects. Environ. Plann. B: Plann. Des.. 41 (6), 1006–1021.

Downs, J., Horner, M., Lamb, D., et al., 2018. Testing time-geographic density estimation for home range analysis using an agent-based model of animal movement. Int. J. Geograph. Inform. Sci. 32 (7), 1505–1522.

Furtado, A.S., et al., 2018. Unveiling movement uncertainty for robust trajectory similarity analysis. Int. J. Geograph. Inform. Sci. 32 (1), 140–168.

Gogate, U., Bakal, J.W., 2016. Smart healthcare monitoring system based on wireless sensor networks. In: 2016 International Conference on Computing, Analytics and Security Trends (CAST). IEEE. 594-599.

Hwang, I., Jang, Y.J., 2017. Process mining to discover shoppers' pathways at a fashion retail store using a WiFi-base indoor positioning system. IEEE Trans. Autom. Sci. Eng. 14 (4), 1786–1792.

Kuijpers, B., Miller, H.J., Neutens, T., et al., 2010. Anchor uncertainty and space-time prisms on road networks. Int. J. Geograph. Inform. Sci. 24 (8), 1223–1248.

Kwan, M.P., 1998. Space-time and integral measures of individual accessibility: a comparative analysis using a point-based framework. Geograph. Anal. 30 (3), 191–216.

Li, H., et al., 2018. In search of indoor dense regions: An approach using indoor positioning data. IEEE Trans. Knowl. Data Eng. 30 (8), 1481–1495.

Li, Z., Zhao, X., Zhao, Z., et al., 2021. WiFi-RITA positioning: Enhanced crowdsourcing positioning based on massive noisy user traces. IEEE Trans. Wireless Commun. 20 (6), 3785–3799.

Liu, T., Kuang, J., Ge, W., et al., 2020. A simple positioning system for large-scale indoor patrol inspection using foot-mounted INS, QR code control points, and smartphone. IEEE Sens. J. 21 (4), 4938–4948.

Liu, Z., Wang, A., Weber, K., et al., 2022a. Categorisation of cultural tourism attractions by tourist preference using location-based social network data: The case of Central, Hong Kong. Tourism Manage. 90, 104488.

Liu, Z., Shi, W., Yu, Y., et al., 2022b. A LSTM-based approach for modelling the movement uncertainty of indoor trajectories with mobile sensing data. Int. J. Appl. Earth Observ. Geoinform. 108, 102758.

Lu, H., et al., 2016. Finding Frequently Visited Indoor POIs Using Symbolic Indoor Tracking Data. ed. EDBT. 449-460.

Miller, H.J., 1991. Modelling accessibility using space-time prism concepts within geographical information systems. Int. J. Geograph. Inform. Sci. 5 (3), 287–301.

Munzert, S., Selb, P., Gohdes, A., et al., 2021. Tracking and promoting the usage of a COVID-19 contact tracing app. Nat. Human Behav. 5 (2), 247–255.

Pal, D., Funilkul, S., Charoenkitkarn, N., et al., 2018. Internet-of-things and smart homes for elderly healthcare: An end user perspective. IEEE Access 6, 10483–10496.

Pfoser, D., Jensen, C.S., 1999. Capturing the uncertainty of moving-object representations. ed. International Symposium on Spatial Databases. 111-131.

Pfoser, D., Jensen, C.S., 1999. Capturing the uncertainty of moving-object representations. ed. In: International Symposium on Spatial Databases. 111-131.

Renaudin, V., Ortiz, M., Perul, J., et al., 2019. Evaluating indoor positioning systems in a shopping mall: The lessons learned from the IPIN 2018 competition. IEEE Access 7, 148594–148628.

Ridel, D., Rehder, E., Lauer, M., et al., 2018. A literature review on the prediction of pedestrian behavior in urban scenarios. 21st International Conference on Intelligent Transportation Systems (ITSC). IEEE. 3105-3112.

Shi, W., Chen, P., Shen, X., et al., 2021. An adaptive approach for modelling the movement uncertainty in trajectory data based on the concept of error ellipses. Int. J. Geograph. Inform. Sci. 35 (6), 1131–1154.

Shi, W., Zeng, F., Zhang, A., et al., 2022. Online public opinion during the first epidemic wave of COVID-19 in China based on Weibo data. Humanities Soc. Sci. Commun. 9 (1), 1–10.

Shu, X., Zhang, L., Sun, Y., et al., 2020. Host–parasite: graph LSTM-in-LSTM for group activity recognition. IEEE Trans. Neural Networks Learn. Syst. 32 (2), 663–674.

Weiser, M., 1991. The Computer for the 21st Century. Sci. Am. 265 (3), 94–104.

Xia, F., Wang, J., Kong, X., et al., 2018. Exploring human mobility patterns in urban scenarios: A trajectory data perspective. IEEE Commun. Mag. 56 (3), 142–149.

Yu, Y., Chen, R., Chen, L., et al., 2020. Precise 3-D indoor localization based on Wi-Fi FTM and built-in sensors. IEEE Internet Things J. 7 (12), 11753–11765.

Yu, Y., Chen, R., Chen, L., et al., 2021. Autonomous 3d indoor localization based on crowdsourced wi-fi fingerprinting and mems sensors. IEEE Sens. J. 22 (6), 5248–5259.

Yu, Y., Chen, R., Shi, W., et al., 2022a. Precise 3D Indoor Localization and Trajectory Optimization Based on Sparse Wi-Fi FTM Anchors and Built-In Sensors. IEEE Trans. Veh. Technol. 71 (4), 4042–4056.

Yu, Z., Lu, Y., An, Q., et al., 2022b. Real-Time Multiple Gesture Recognition: Application of a Lightweight Individualized 1D CNN Model to an Edge Computing System. IEEE Trans. Neural Syst. Rehabil. Eng. 20, 990–998.

Zheng, K., et al., 2012. Reducing uncertainty of low-sampling-rate trajectories. In: 2012 IEEE 28th International Conference on Data Engineering. Arlington, Virginia, pp. 1144–1155.

Zheng, Y., 2015. Trajectory data mining: an overview. ACM Trans. Intell. Syst. Technol. (TIST). 6 (3), 29.

Zheng, Z., Rasouli, S., Timmermans, H., 2014. Evaluating the accuracy of GPS-based taxi trajectory records. Procedia Environ. Sci. 22, 186–198.

Zhou, X., Luo, Q., Zhang, D., et al., 2018. Detecting taxi speeding from sparse and low-sampled trajectory data. In: Asia-Pacific Web (APWeb) and Web-Age Information Management (WAIM) Joint International Conference on Web and Big Data. Springer, Cham, pp. 214–222.

Zhou, B., Ma, W., Li, Q., et al., 2021. Crowdsourcing-based indoor mapping using smartphones: A survey. ISPRS J. Photogramm. Remote Sens. 177, 131–146.

Zhu, F., Lv, Y., Chen, Y., et al., 2019. Parallel transportation systems: Toward IoT-enabled smart urban traffic control and management. IEEE Trans. Intell. Transp. Syst. 21 (10), 4063–4071.